Partial rupture of a locked patch of the Sumatra megathrust during the 2007 earthquake sequence

Konca, A. Ozgun; Avouac, Jean-Philippe; Sladen, Anthony; Meltzner, Aron J.; Sieh, Kerry; Fang, Peng; Li, Zhenhong; Galetzka, John; Genrich, Jeff; Chlieh, Mohamed; Natawidjaja, Danny H.; Bock, Yehuda; Fielding, Eric J.; Ji, Chen; Helmberger, Don V.

2008

Konca, A. O., Avouac, J. P., Sladen, A., Meltzner, A. J., Sieh, K., Fang, P., et al. (2008). Partial rupture of a locked patch of the Sumatra megathrust during the 2007 earthquake sequence. Nature, 456, 631-635.

https://hdl.handle.net/10356/95454

https://doi.org/10.1038/nature07572

Partial rupture of a locked patch of the Sumatra megathrust during the 2007 earthquake sequence

A. Ozgun Konca[1], Jean-Philippe Avouac[1], Anthony Sladen[1], Aron J. Meltzner[1], Kerry Sieh [1]†, Peng Fang[2], Zhenhong Li[3], John Galetzka[1], Jeff Genrich[1], Mohamed Chlieh[4], Danny H. Natawidjaja[1], Yehuda Bock[2], Eric J. Fielding[5], Chen Ji[6] & Don V. Helmberger[1]

[1]Tectonics Observatory, Division of Geological and Planetary Sciences, California Institute of Technology, Pasadena, California 91125, USA.

[2]Scripps Institution of Oceanography, University of California, San Diego, La Jolla, California 92093, USA.

[3]COMET, Department of Geographical and Earth Sciences, University of Glasgow, Glasgow G12 8QQ, UK.

[4]Geosciences Azur, Université de Nice Sophia-Antipolis, Institut de Recherche pour le Développement, Observatoire de la Cote d'Azurrue, 06560 Valbonne, France.

[5]Jet Propulsion Laboratory, M.S. 300-233, California Institute of Technology, Pasadena, California 91109, USA.

[6]Department of Geological Sciences, University of California, Santa Barbara, California 94106.

†Present address: Earth Observatory of Singapore, Nanyang Technological University, 50 Nanyang Avenue, 639798 Singapore.

Correspondence and requests for materials should be addressed to J.-P.A. (avouac@gps.caltech.edu).

The great Sumatra–Andaman earthquake and tsunami of 2004 was a dramatic reminder of the importance of understanding the seismic and tsunami hazards of subduction zones[1–4]. In March 2005, the Sunda megathrust ruptured again, producing an event[5] of moment magnitude (M_w) 8.6 south of the 2004 rupture area, which was the site of a similar event in 1861 (ref. 6). Concern was then focused on

the Mentawai area, where large earthquakes had occurred in 1797 (M_w=8.8) and 1833 (M_w=9.0)[6,7]. Two earthquakes, one of M_w=8.4 and, twelve hours later, one of M_w=7.9, indeed occurred there on 12 September 2007. Here we show that these earthquakes ruptured only a fraction of the area ruptured in 1833 and consist of distinct asperities within a patch of the megathrust that had remained locked in the interseismic period. This indicates that the same portion of a megathrust can rupture in different patterns depending on whether asperities break as isolated seismic events or cooperate to produce a larger rupture. This variability probably arises from the influence of non-permanent barriers, zones with locally lower pre-stress due to the past earthquakes. The stress state of the portion of the Sunda megathrust that had ruptured in 1833 and 1797 was probably not adequate for the development of a single large rupture in 2007. The moment released in 2007 amounts to only a fraction both of that released in 1833 and of the deficit of moment that had accumulated as a result of interseismic strain since 1833. The potential for a large megathrust event in the Mentawai area thus remains large.

Slip along a subduction megathrust can be either aseismic or seismic. Seismic slip commonly has a duration of seconds to minutes, with sliding velocities of about a metre per second and rupture velocities of a few kilometres per second[8]. Such rapid failure generates strong ground shaking and tsunamis. Slower, aseismic slip is also common, and dominates at depths greater than about 40km (ref. 9) but also occurs at shallower depths[10–14]. This process leads to heterogeneous strain accumulation in the interseismic period, with stress building up around locked patches that presumably fail during megathrust earthquakes.

The modelling of geodetic and palaeogeodetic measurements of interseismic strain indeed shows that the Sunda megathrust, off the shore of Sumatra, consists of a patchwork of creeping and locked areas[15] (Fig. 1) and suggests some correlation between megathrust earthquakes and interseismic coupling. A recent example of this is the rupture of a 350-km section, in the 2005, M_w=8.6 Nias earthquake[5]. Historical accounts[6] and palaeoseismic data[16] indicate that rupture of almost the same patch produced an earlier great earthquake in 1861. Immediately south of the Nias patch, near the Equator,

coupling is low and consistent with there having been only moderate earthquakes in the past few centuries[10,17]. Farther south, beneath the Mentawai Islands, coupling has been high for at least the past 40 years and great earthquakes have occurred there[18]. These observations indicate that the pattern of interseismic strain accumulation has a strong influence on the characteristics of large megathrust ruptures.

Nonetheless, successive seismic ruptures in the same area may differ significantly in extent and magnitude[19–21]. This Letter provides a very well-documented case of such variability. We show that the 2007 sequence of large seismic ruptures on the strongly coupled Mentawai patch differs significantly from previous ruptures of this section in 1833 and 1797. The slip and extent of the recent ruptures are much smaller than during those previous events. Moreover, the amount of moment released during the recent events is much less than the deficit of moment that has accumulated since the previous great earthquakes.

We use Global Positioning System (GPS) measurements, field measurements of uplift, synthetic aperture radar (SAR) interferometry (InSAR) and seismological records to estimate the source parameters of the two large earthquakes of 12 September 2007. Details are given in Supplementary Information. The 2007 ruptures occurred beneath a large subset of the continuously recording GPS (cGPS) stations of the Sumatran GPS array. Displacements assigned to each of the events were determined from 120-s time series. By contrast, the InSAR and field measurements provide information only on the cumulative effects of the sequence of earthquakes. These measurements cover greater lengths of time and therefore must include some amount of postseismic deformation as well.

All horizontal GPS motions are trenchwards (Fig. 2a). The maximum horizontal displacement due to the cumulative effect of the whole sequence, 1.5 m, occurred at station BSAT on South Pagai Island. Vertical displacements were measured at the GPS stations and from the emergence or submergence of coral microatolls on the reefs that fringe the Mentawai Islands. They show uplift of the islands and subsidence of the mainland coast (Fig. 2a, inset). The maximum uplift reaches 1.3 m on Mega Island, about

70km northwest of the epicentre. Uplift decreases northwards to about 1 m on southern South Pagai Island to 10 cm on North Pagai Island. Uplift at Sipora Island is on the order of 20 cm. These data are complemented with InSAR line-of-sight displacements. Using ROI_PAC (repeat-orbit interferometry package) software[22], we processed four independent interferograms from phased-array-type L-band SAR (PALSAR) images acquired by the Advanced Land Observing Satellite (Japan Aerospace Exploration Agency). These data are consistent with the GPS and coral measurements where they coincide, and provide a much denser spatial coverage. They show a strong displacement gradient under the Pagai Islands and reveal a zone of deformation beneath an area north of Bengkulu on mainland Sumatra (Supplementary Fig. 1).

We determine static and kinematic source models from the modelling of the surface displacements and teleseismic waveforms recorded at a selection of IRIS (Incorporated Research Institutions for Seismology) stations chosen to ensure good azimuthal coverage. The geometry of the megathrust is approximated by a plane dipping 15 ° to the northeast, away from the trench. We also derive models that feature a curved fault geometry with the dip angle increasing with depth (Supplementary Information). These tests show that the results described here are independent of the assumed geometry of the megathrust. We first derived a cumulative slip model that includes the M_w=8.4 and M_w=7.9 earthquakes using the cGPS cumulative displacements, the field measurements of uplift and the InSAR data. The model obtained using only the cGPS displacements measured from just before the M_w=8.4 event until just after the M_w=7.9 event is the least contaminated by postseismic relaxation. It suggests that there is a relatively patchy slip distribution with a geodetic moment of 7.3×10^{21} Nm (Supplementary Fig. 2a). The spatial resolution of the model improves when the InSAR and field data are added, but some contamination by postseismic deformation is introduced. The best-fitting model calculated from all these data (Fig. 2a) has a total moment of 7.5×10^{21} Nm (equivalent to M_w=8.5), which is only marginally larger than that derived from the cGPS measurements alone. Thus, we consider this source model to be a better-constrained representation of the coseismic slip distribution than the model derived from only GPS data. This cumulative source model is also very similar to that obtained by summing the M_w=8.4 and M_w=7.9 models and a M_w=7.0 aftershock model (Supplementary Fig. 2b).

The greater resolution afforded by the coral and InSAR measurements shows that the patchiness of the slip distribution is real and not an artefact of our methodology.

The cumulative slip model (Fig. 2a) has a dumb-bell-shaped principal rupture area extending contiguously northwestwards from the hypocentre, off the shore of Bengkulu, to South Pagai Island. In addition, there are two disconnected minor slip patches. One is below northern Sipora Island, about 100 km along the strike direction of the northwestern edge of the principal rupture. The other lies beneath the volcanic arc of the mainland, about 100 km down-dip from the down-dip edge of the principal rupture. Slip peaks at 8 m on the main patch under southern South Pagai Island and at 5-m local maxima about 25 km northeast of Mega Island. The maximum slip on the small patch beneath Sipora Island is 2.5 m. All data sets are fitted well by slip on a single plane representing the megathrust; slip on any other fault is therefore not required.

We also derived separate kinematic source models of the mainshock and principal aftershock using teleseismic waveforms, GPS measurements and subsets of the coral and InSAR data. For this analysis, we discarded data from the Pagai Islands, where the contributions from each of the two events cannot be distinguished. Farther south and east, the displacements measured along PALSAR track 445 and coral measurements on Mega Island are clearly attributable to the mainshock alone (Supplementary Information, section H). We modelled these subsets of the coral and InSAR data together with the GPS measurements and the teleseismic records of the mainshock.

The source model of the M_w=8.4 mainshock shows unilateral northward rupture, which started about 70 km south of Mega Island (Fig. 2b). As in the cumulative source model, the most prominent slip loci are under southern South Pagai Island, where slip peaks at about 7 m; about 25 km north of Mega Island, where slip peaks at about 6 m; and on the deep patch east of the Sumatran coast (Fig. 1, inset). The total seismic moment of this model ($\sim 5 \times 10^{21}$ Nm) is consistent with the Global Centroid Moment Tensor moment magnitude (http://www.globalcmt.org/). The source time function indicates that the rupture was not very impulsive and lasted for about 100s (Fig. 2b, inset). The rise times are estimated to be 5–10s, and the moment rate increased smoothly over the first 20s

(Supplementary Fig. 5). The southern patch slipped during the first 40s and the northern patch slipped during the second 40s.

The model of the M_w=7.9 earthquake derived from the joint inversion of the teleseismic and cGPS data shows that this earthquake also involved failure of more than one discrete patch (Fig. 2c). The moment of this event, 1.1×10^{21} N m, was released in two pulses over about 80s. (Fig. 2c, inset). Rupture began within a few kilometres of the down-dip edge of the mainshock's northern patch. The seismic waveforms require an extremely abrupt initiation of the first subevent (rise times of a few seconds at most) and a highly peaked slip distribution around the hypocentre. The second subevent occurred in 50– 80s and about 130km farther northwest of the epicentre, east of northeastern Sipora Island. There is no evidence for significant slip between these two subevents.

The September 2007 sequence ruptured a number of distinct asperities (defined here as patches with locally large slip) on the megathrust that lie both within a patch that had remained strongly locked in the interseismic period and within the rupture area of the 1833 earthquake (Fig. 1). However, the patterns and amounts of slip in 1833 and 2007 are significantly different. Coseismic uplifts in 1833 (between 1 and 2.5 m from South Pagai Island to Sipora Island)[7], are much larger than those observed in 2007. This is consistent with the cumulative geodetic moment of 7.5×10^{21} Nm released by the 2007 earthquake sequence, representing a fraction of the moment of $(10– 55) \times 10^{21}$Nm released in 1833 (ref. 15; Fig. 3). The coast of North Pagai Island was uplifted by 2.2 min 1833 (ref. 7). This area is clearly a low-slip patch in 2007, as indicated by the modest horizontal and vertical displacements recorded at station SLBU (22cm and 7cm, respectively). Thus, it acted more like a 'barrier' during the coseismic slip in 2007.

South of latitude 2 ° S, the moment deficit accumulated since 1833 is still less than the moment released during the 1797 and 1833 events (Fig. 3). North of this latitude, the accumulated deficit is far greater than the moment released during the 1797 and 1833 events. Thus, the next great rupture might have been expected to occur north of 2 ° S; instead, the 2007 events occurred south of 2 °S. Furthermore, the moment released during the 2007 sequence is much less than that released during the 1833 event and much less

than that which has accumulated since then. These relationships clearly demonstrate that the Mentawai patch is behaving in neither a slip- nor a time-predictable manner. If rupture were time predictable, slip would already have occurred north of 2 °S. If rupture were slip predictable, slip would have been far greater in 2007 south of 2 °S.

Two salient questions are why the 2007 sequence did not duplicate the 1833 event and why it released only about 25% of the deficit of moment that had accumulated since 1833. The 2007 sequence consisted of several spatially and temporally separate asperities that probably did not cooperate effectively. If two neighbouring asperities on the same fault plane rupture jointly, they are expected to cooperate to release more moment than if they had ruptured independently[23]. This is because the static stress change induced by one asperity increases both the stress on the other and, hence, the elastic stress that is released during the rupture.

Spatio-temporal evolutions of the 2007 ruptures show that this kind of cooperation was not effective. For example, slip on the second asperity of the M_w=7.9 earthquake (2B in Fig. 1; see inset for all labelled asperities) started only once the slip on the first asperity (2A) was over. The reloading of asperity 2A due to rupture of asperity 2B thus did not contribute to any additional slip. This may be because the area between the two asperities acted as a barrier to rupture propagation. This intervening area beneath North Pagai Island experienced little coseismic slip in 2007, but is probably not a permanent barrier, because the same area is predicted to have experienced the largest cumulative slip (of about 17 m) by the sum of the slip models of the 1797 and 1833 earthquakes[7]. This area may therefore have acted as a barrier in 2007 because it had a locally lower stress level before the earthquake, as a result of release during previous earthquakes. Minimal cooperation between the rupture of asperities 1B and 2A is also evident from the 12-h time lag between their ruptures. The cause of the lack of cooperation between these two asperities is more enigmatic, given that they lie so close to each other. A narrow zone with low pre-stress due to the slip distribution related to the 1833 and 1797 events may have acted as a barrier, or there may be a creeping zone too narrow to be seen in the pattern of interseismic strain. In any case, it appears that the static stress increase on asperity 2A due to the M_w=8.4 earthquake was enough to trigger a delayed rupture of this

asperity. By contrast, the dynamic stresses induced by the M_w=8.4 earthquake failed to trigger the rupture of asperity 2A.

Two independent SAR interferograms and the GPS displacement at station LAIS show that the M_w=8.4 rupture induced a localized surface deformation just north of Bengkulu, and that this deformation took place during the earthquake, even though it did not contribute much to the seismic radiation (Supplementary Information). It is possible to model this signal as a deep slip patch on the megathrust that falls in a zone that creeps in the interseismic period (asperity 1C). Because this slip patch is isolated, we exclude the possibility that it is a result of the rupture propagating into the rate-strengthening zones. It could reflect seismic rupture of a rate-weakening portion of the megathrust embedded in a dominantly creeping zone, or it may be an example of a triggered aseismic transient. Deep aseismic transients on megathrusts have been observed[14] and justified on the basis of rate and state friction theory[24,25]. Another possibility is that this deformation did not take place on the megathrust but at lesser depths. The available data do not resolve this ambiguity.

In conclusion, the rupture area of the 2007 Mentawai earthquakes was confined to a subset of a locked portion that is surrounded by creep during the interseismic period. Such permanent barriers, which are found to influence the down-dip extent as well as the lateral extent of megathrust ruptures, can be imaged from the modelling of interseismic strain[2,12–15] except when they lie in stress shadows, in particular along the up-dip portion of the plate interface[11]. The complex spatio-temporal pattern of the 2007 rupture is probably related to the fact that it produced much less slip than did historical earthquakes in the area. The 2007 ruptures released only 25% of the deficit of moment that had accumulated since the last rupture. The sequence essentially ruptured a set of asperities, which triggered each other through static and dynamic interactions but did not cooperate efficiently, because of the intervening barriers. Some of these barriers are most likely not permanent and are related to the slip in past earthquakes. Whereas permanently creeping barriers should tend to favour some regularity and similarity of earthquakes, the presence of non-permanent barriers due to the stress distribution left over from previous ruptures is probably the major factor introducing irregularity, as observed in dynamic fault

models[26,27]. This is probably the main reason that neither the slip-predictable nor the time-predictable models apply, and why the 2007 earthquakes did not grow as big as the 1833 earthquake. This supports the view that seismic asperities are probably not permanent features[28] but rather move from one rupture to another within the area that is locked in the interseismic period.

METHODS SUMMARY

We assume that the seismic rupture can be modelled as the propagation of a rupture front with finite width. The kinematic source model is then characterized by the static slip, the rupture velocity and the rise time, namely the time it takes for slip at a point on the fault to reach its final static displacement, at each elementary patch. The joint inversion consists of searching for the model that best fits the wavelet transform of the seismograms, the geodetic data and the InSAR data. We use an optimization method based on a simulated annealing algorithm, where bounded parameter spaces of slip amplitude, rake angle and rupture velocity are searched to obtain models that fit both teleseismic and geodetic data[29]. Rupture velocity is allowed to vary between 2.1 and 2.8 km s^{-1}, and the rake angle can vary between 80 ° and 130 °. We selected teleseismic waveforms from the IRIS network to ensure good azimuthal coverage, constraining the source model. The broadband seismograms were bandpass filtered from 1.5 s (P waves) and 3 s (SH waves) to 200 s. We used 16 P and 19 SH waveforms for the M_w=8.4 earthquake and 19 P and 17 SH waveforms for the M_w=7.9 earthquake. The duration of the waveforms used for modelling the earthquake was 120 s for both the M_w=8.4 earthquake and the M_w=7.9 earthquake. Details on the GPS and InSAR data and the inversion method are given in Supplementary Information.

Acknowledgements

This study was partly funded by the NSF (grant EAR-0538333) and the Gordon and Betty Moore Foundation. This is Caltech Tectonics Observatory contribution no.93. We thank R. Burgmann for comments and suggestions.

References

1. Lay, T. *et al*. The great Sumatra-Andaman earthquake of 26 December 2004. Science **308**, 1127–1133 (2005).

2. Chlieh, M. *et al*. Coseismic slip and afterslip of the great M_w 9.15 Sumatra-Andaman earthquake of 2004. *Bull. Seismol. Soc. Am.* **97**, S152–S173 (2007).

3. Ammon, C. J. *et al*. Rupture process of the 2004 Sumatra-Andaman earthquake. *Science* **308**, 1133–1139 (2005).

4. Subarya, C. *et al*. Plate-boundary deformation associated with the great Sumatra-Andaman earthquake. *Nature* **440**, 46–51 (2006).

5. Briggs, R. W. *et al*. Deformation and slip along the Sunda Megathrust in the great 2005 Nias-Simeulue earthquake. *Science* **311**, 1897–1901 (2006).

6. Newcomb, K. & McCann, W. Seismic history and seismotectonics of the Sunda arc. *J. Geophys. Res.* **92**, 421–439 (1987).

7. Natawidjaja, D. H. *et al*. Source parameters of the great Sumatran megathrust earthquakes of 1797 and 1833 inferred from coral microatolls. *J. Geophys. Res.* **111**, doi:10.1029/2005JB004025 (2006).

8. Ruff, L. & Kanamori, H. Seismic coupling and uncoupling at subduction zones. *Tectonophysics* **99**, 99–117 (1983).

9. Pacheco, J. F., Sykes, L. R. & Scholz, C. H. Nature of seismic coupling along simple plate boundaries of the subduction type. *J. Geophys. Res.* **98**, 14133–14160 (1993).

10. Sieh, K., Ward, S. N., Natawidjaja, D. & Suwargadi, B. W. Crustal deformation at the Sumatran subduction zone revealed by coral rings. *Geophys. Res. Lett.* **26**, 3141–3144 (1999).

11. Burgmann, R. *et al*. Interseismic coupling and asperity distribution along the Kamchatka subduction zone. *J. Geophys. Res.* **110**, doi:10.1029/2005JB003648

(2005).

12. Suwa, Y., Miura, S., Hasegawa, A., Sato, T. & Tachibana, K. Interplate coupling beneath NE Japan inferred from three-dimensional displacement field. *J. Geophys. Res.* **111**, doi:10.1029/2004JB003203 (2006).

13. Freymueller, J. T. & Beavan, J. Absence of strain accumulation in the western Shumagin segment of the Alaska subduction zone. *Geophys. Res. Lett.* **26**, 3233–3236 (1999).

14. Pritchard, M. E. & Simons, M. An aseismic slip pulse in northern Chile and along-strike variations in seismogenic behavior. *J. Geophys. Res.* **111**, doi:10.1029/2006JB004258 (2006).

15. Chlieh, M., Avouac, J.-P., Sieh, K., Natawidjaja, D. H. & Galetzka, J. Heterogeneous coupling on the Sumatra megathrust constrained from geodetic and paleogeodetic measurements. *J. Geophys. Res.* **113**, doi:10.1029/2007JB004981 (2008).

16. Meltzner, A. J. *et al*. Coseismic, postseismic, and interseismic deformation, and long-term segmentation near the boundary of the 2004 and 2005 Sunda megathrust ruptures. *Eos* **88** (Fall meeting), abstr. S24A-02 (2007).

17. Natawidjaja, D. *et al*. Paleogeodetic records of seismic and aseismic subduction from central Sumatran microatolls, Indonesia. *J. Geophys. Res.* **109**, doi:10.1029/2003JB0002398 (2004).

18. Natawidjaja, D. H. *et al*. Interseismic deformation above the Sunda Megathrust recorded in coral microatolls of the Mentawai islands, West Sumatra. *J. Geophys. Res.* **112**, doi:10.1029/2006JB004450 (2007).

19. Thatcher, W. Order and diversity in the modes of Circum-Pacific earthquake recurrence. *J. Geophys. Res.* **95**, 2609–2623 (1990).

20. Ando, M. Source mechanisms and tectonic significance of historical earthquakes along Nankai Trough, *Japan. Tectonophysics* **27**, 119–140 (1975).

21. Lay, T., Kanamori, H. & Ruff, L. The asperity model and the nature of large subduction zone earthquakes. *Earthq. Predict. Res.* **1**, 3–71 (1982).

22. Rosen, P. A., Henley, S., Peltzer, G. & Simons, M. Updated repeat orbit interferometry package released. *Eos* **85**, 47 (2004).

23. Rundle, J. B. & Kanamori, H. Application of an inhomogeneous stress (patch) model to complex subduction zone earthquakes - a discrete interaction matrix approach. *J. Geophys. Res.* **92**, 2606–2616 (1987).

24. Perfettini, H. & Ampuero, J. P. Dynamics of a velocity strengthening fault region: Implications for slow earthquakes and postseismic slip. *J. Geophys. Res.* **113**, doi:10.1029/2007JB005398 (2008).

25. Liu, Y. & Rice, J. R. Aseismic slip transients emerge spontaneously in three-dimensional rate and state modeling of subduction earthquake sequences. *J. Geophys. Res.* **110**, B08307 (2005).

26. Ben-Zion, Y. & Rice, J. R. Earthquake failure sequences along a cellular fault zone in a 3-dimensional elastic solid containing asperity and nonasperity regions. *J. Geophys. Res.* **98**, 14109–14131 (1993).

27. Cochard, A. & Madariaga, R. Complexity of seismicity due to highly rate-dependent friction. *J. Geophys. Res.* **101**, 25321–25336 (1996).

28. Park, S. C. & Mori, J. Are asperity patterns persistent? Implication from large earthquakes in Papua New Guinea. *J. Geophys. Res.* **112**, doi:10.1029/ 2006JB004481 (2007).

29. Ji, C., Wald, D. & Helmberger, D. V. Source description of the 1999 Hector Mine, California earthquake, Part I: Wavelet domain inversion theory and resolution analysis. *Bull. Seismol. Soc. Am.* **92**, 1192–1207 (2002).

30. Abercrombie, R. E., Antolik, M. & Ekstrom, G. The June 2000 M_w 7.9 earthquakes south of Sumatra: Deformation in the India-Australia Plate. *J. Geophys. Res.* **108**,

List of Figures

Figure 1 **Patches with strong interseismic coupling on the Sunda megathrust coincide with large seismic ruptures.** The pattern of coupling, defined as the ratio of interseismic slip rate to plate convergence rate, is derived from the modelling of geodetic and paleogeodetic data[15]. No information is available on coupling under northern Simeulue, west of about 96.2 ° E. The black arrow shows the 5.7 cm yr^{-1} plate convergence rate. Slip distribution of the M_w=8.6 earthquake of 2005 is shown using 5-m contour lines in green[5]. Gray and black polygons show estimated rupture areas of the 1797 and 1833 earthquakes[7]. Dark and pale blue lines show the 1-m and 5-m slip contour lines of the M_w=8.4 and M_w=7.9 seismic ruptures of 2007, respectively; stars show the epicentres. The smaller, M_w=7.7, earthquake of 1935 (ref. 17) occurred in a region of weak coupling. The M_w=7.9 earthquake of 2000, which is predominantly an intraslab strike-slip event[30] also falls in an area with low coupling. The inset map displays various asperities of the 2007 rupture sequence.

Figure 2 **Models of megathrust slip during the M_w=8.4 and M_w=7.9 earthquakes show principal slip on widely separated patches.** All slip models and GPS vectors are plotted on the scale represented by the 50-cm arrow. Slip contour lines are plotted every 1 m, starting at 1 m. **a**, Cumulative slip distribution due to the M_w=8.4 and M_w=7.9 earthquakes of 12 September 2007. Contours show cumulative slip of best-fitting inversion of the GPS, coral and InSAR data. Vectors show observed (black) and modelled (green) horizontal displacement values at cGPS stations of the Sumatran GPS array (http://www.tectonics.caltech.edu). Normalized error ellipses are also shown. Inset, vertical GPS displacements and measurements of coral uplift (black) and the fits from the model (GPS, green; coral, red). **b**, Slip model of the M_w=8.4 earthquake obtained from the joint inversion of teleseismic waveforms, GPS data, InSAR data and measurements of coral uplift unambiguously attributable to the M_w=8.4 event. Observed displacements,

shown with error ellipses in black, originate at the GPS station locations and coral sites. Modelled horizontal and vertical vectors are green and red, respectively. Red stars represent the locations of epicentre as accepted by the US Geological Survey. Inset, moment rate function. Geodetic data are tabulated and fits to the InSAR and teleseismic data are shown in Supplementary Information. **c**, Model of the M_w=7.9 earthquake from the joint inversion of teleseismic waveforms and GPS measurements. Vector colour coding is the same as in **b**. Inset, the moment rate function shows that the moment was released in two discrete episodes, about 20s apart. Fits to the teleseismic data are shown in the Supplementary Information.

Figure 3 **Comparison of the moment released in 2007 with the moment deficit accumulated since the 1797 and 1833 earthquakes.** Light grey curves are the upper and lower bounds of estimated moment release for the 1833 and 1797 earthquakes, based on modelling of geodetic and paleogeodetic data[15] and taking into account the effect of 20% postseismic slip. The confidence intervals were deduced from the uncertainties in the extent of the ruptures and in the eventual contribution of postseismic deformation to the vertical displacements deduced from the coral data. The purple curve shows accumulated moment deficit since the last great rupture, derived from the modelling of interseismic strain accumulation (Fig. 1, model J-a of ref. 15). Moment deficit values are integrals within bins that are one-half degree of latitude wide.

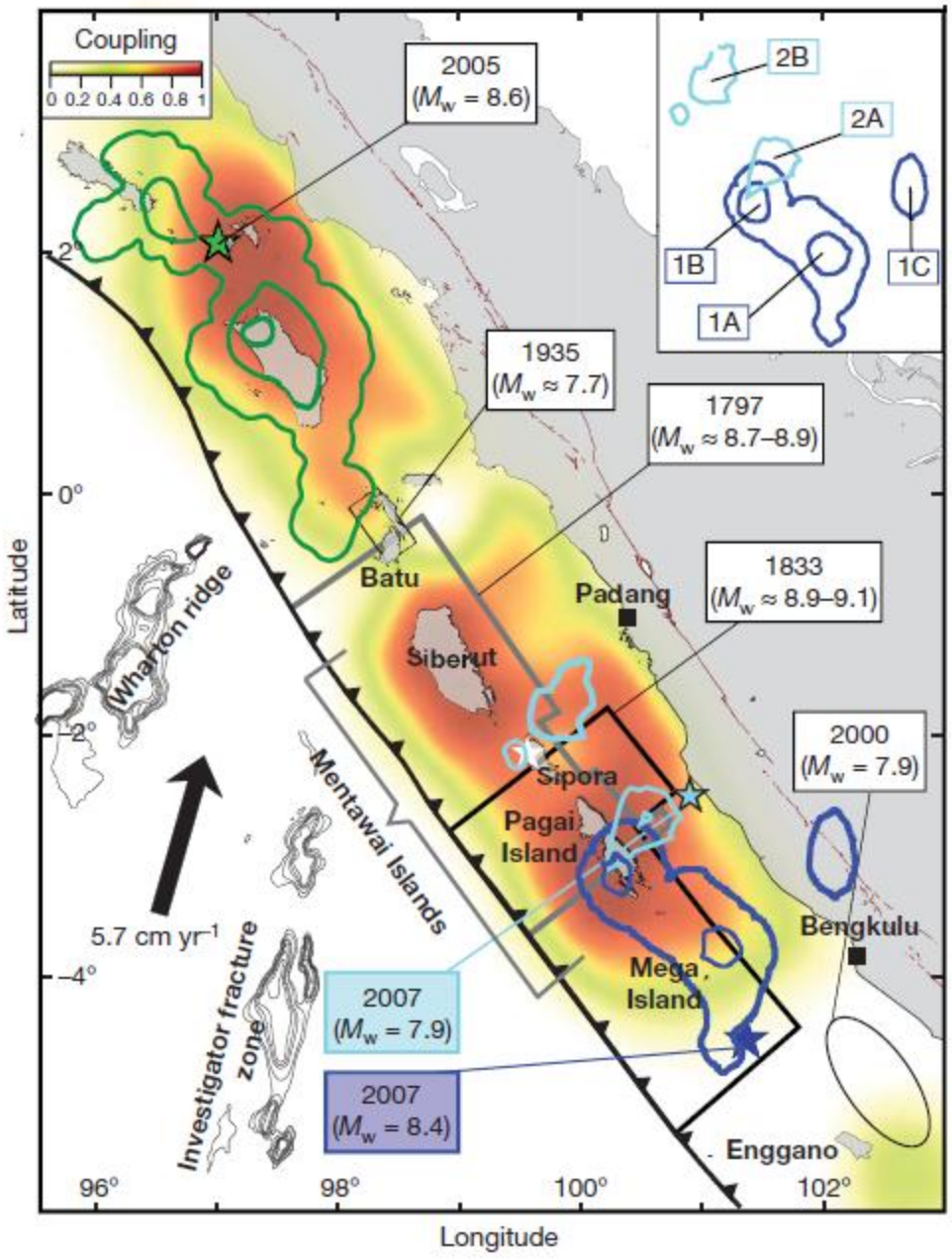
Coupling
0 0.2 0.4 0.6 0.8 1
2005
(M_w = 8.6)
2B
2A
1B
1C
1A
1935
(M_w ≈ 7.7)
1797
(M_w ≈ 8.7–8.9)
1833
(M_w ≈ 8.9–9.1)
2000
(M_w = 7.9)
2007
(M_w = 7.9)
2007
(M_w = 8.4)
Batu
Padang
Siberut
Sipora
Pagai Island
Mega Island
Bengkulu
Enggano
Mentawai Islands
Wharton ridge
Investigator fracture zone
5.7 cm yr^{-1}
2°
0°
–2°
–4°
96°
98°
100°
102°
Latitude
Longitude

Figure 1

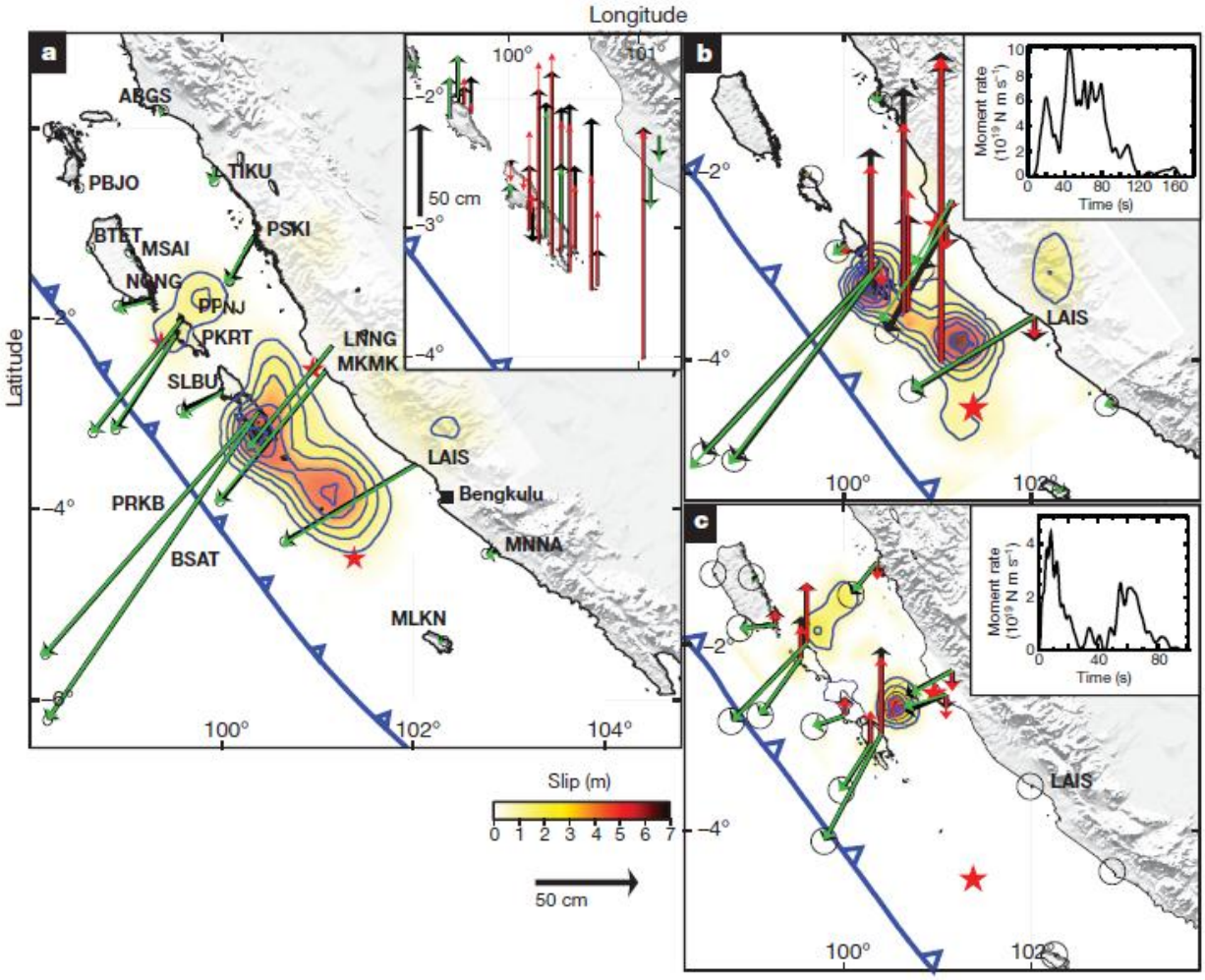
Longitude
Latitude
a
b
c
ABGS
PBJO
TIKU
PSKI
BTET
MSAI
NGNG
PPNJ
PKRT
LNNG
MKMK
SLBU
LAIS
Bengkulu
PRKB
BSAT
MNNA
MLKN
50 cm
Slip (m)
0 1 2 3 4 5 6 7
Moment rate
Time (s)
100°
101°
102°
104°
−2°
−3°
−4°
−6°

Figure 2

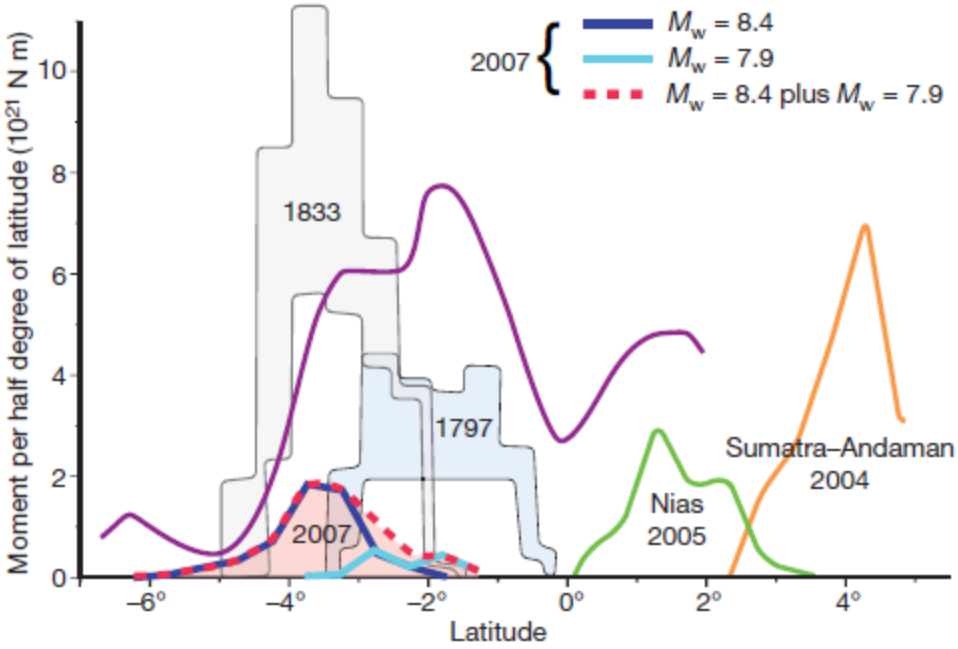
2007
M_w = 8.4
M_w = 7.9
M_w = 8.4 plus M_w = 7.9
1833
1797
2007
Nias
2005
Sumatra–Andaman
2004
Moment per half degree of latitude (10^{21} N m)
0
2
4
6
8
10
–6°
–4°
–2°
0°
2°
4°
Latitude

Figure 3